International Journal of Computer Information Systems and Industrial Management Applications
ISSN 2150-7988 Volume 18(21s) 2026 pp. 1349-1366
https://doi.org/10.70917/ijcisim-2026-5397
Article

Antifungal efficacy and characterization of the dose-response relationship of Eucalyptus globulus essential oil against Fusarium sp. and Colletotrichum sp. in postharvest fruits of Theobroma cacao

Shellsyn Giraldo Jaramillo[1], Charith Yulieth Jiménez Cepeda[2], Edysabed Riobó Pérez[3]

[1] Programa de Microbiología, Facultad de Ciencias Básicas, Universidad Popular del Cesar, Valledupar, Cesar, Colombia.
Email: shellsyngiraldo@unicesar.edu.co
[2] Programa de Microbiología, Facultad de Ciencias Básicas, Universidad Popular del Cesar, Valledupar, Cesar, Colombia.
Email: cyjimenez@unicesar.edu.co
[3] Programa de Microbiología, Facultad de Ciencias Básicas, Universidad Popular del Cesar, Valledupar, Cesar, Colombia.
Email: eriobo@unicesar.edu.co

Abstract: Postharvest fungal rot caused by Fusarium sp. and Colletotrichum sp. accounts for between 15 and 50% of global Theobroma cacao fruit losses, and conventional synthetic fungicides carry widely documented toxicological and ecological risks. This study evaluated the antifungal potential of Eucalyptus globulus essential oil (EO) as a biofungicide for postharvest cocoa management. The EO was obtained by steam distillation (yield: 1.82 ± 0.14% w/w) and was chemically characterized by gas chromatography coupled to mass spectrometry (CG-MS), confirming a chemotype dominated by 1,8-cineole (72.4 ± 1.7%). In vitro antifungal activity was assessed at five concentrations (0.02–6.30% v/v) using the agar dilution technique; radial growth inhibition percentage (PICR) data were fitted to a four-parameter logistic model (4PL), obtaining EC50 values of 0.96% v/v (95% CI: 0.72–1.28) for Fusarium sp. and 0.36% v/v (95% CI: 0.25–0.52) for Colletotrichum sp. In vivo postharvest efficacy was determined in inoculated cacao fruits by measuring the daily lesion area (cm^2) for 15 days and integrating it into the Area Under the Disease Progression Curve (ABCPE). At the highest dose of AE (≈ CE90), the ABCPE was reduced to 6.9 ± 1.1 $cm^2 \cdot d$ for Fusarium sp. and 5.2 ± 1.0 $cm^2 \cdot d$ for Colletotrichum sp.—values statistically indistinguishable from the reference synthetic fungicide. The integrated approach—which links the chemical identity of EO to nonlinear inhibitory concentrations in vitro and to disease progression metrics in vivo—provides a methodologically rigorous framework for evaluating plant-based biofungicides in tropical postharvest systems.
Keywords: Eucalyptus essential oil; postharvest; Fusarium; Colletotrichum; CE50; ABCPE; 1,8-cineole

1. Introduction

Cocoa (*Theobroma cacao* L.) supports a global value chain valued at tens of billions of dollars annually, although postharvest losses remain a persistent drag on productivity—especially in tropical producing regions where temperature, humidity, and rudimentary storage infrastructure converge to favor fungal colonization. Among the pathogens responsible, *Fusarium* sp. and *Colletotrichum* sp. are the most frequently implicated fruit rot and anthracnose agents, causing estimated losses of between 15 and 50% in postharvest cocoa [Rojo-Báez et al., 2017; Rodríguez-Guzmán et al., 2021]. When considering the broader microbial spoilage—encompassing secondary bacterial and fungal invaders that exploit compromised tissues—total postharvest losses can exceed 80% of harvested fruit (Kanchana et al., 2017; García-Mateos et al., 2023). In the Colombian Caribbean, where cacao cultivation has

expanded rapidly in recent years—from 13 to more than 350 tons marketed by local organizations since 2019—these losses translate directly into reduced incomes for smallholder farmers who rely on cultivation as their primary livelihood strategy (Orozco-Aguilar et al., 2024).

The usual response to postharvest fungal rot has been the application of synthetic fungicides. In Colombia alone, fungicides account for 34.4% of agrochemical imports, and the most widely used active ingredients—tebuconazole, azoxystrobin, mancozeb, pyraclostrobin, and difenoconazole—carry documented risks that extend far beyond target organisms (Chavarro, 2021). Chronic human exposure to these compounds has been linked to endocrine disruption, neurotoxicity, and carcinogenic potential, while environmental monitoring has revealed measurable residues of triazole fungicides and strobilurin in aquatic ecosystems adjacent to agricultural land (Herrera-González et al., 2021). Zubrod et al. [2019] synthesized evidence from multiple freshwater systems demonstrating that fungicide contamination alters decomposing microbial communities, disrupts aquatic food webs, and—paradoxically—can increase pathogen virulence by modifying host immune function. Rohr et al. (2017) documented a specific case of this paradox: the amphibian pathogenic chytrid *Batrachochytrium dendrobatidis* proliferated in the presence of fungicide residues rather than being suppressed by them. These findings call into question the long-term sustainability of a disease management strategy that relies on chemical inputs whose side effects may exacerbate the biological problems they purport to solve.

Plant-based essential oils (AEs) have attracted increasing attention as biofungicide candidates precisely because they offer a different toxicological profile. EOs are complex mixtures of terpenoids, phenylpropanoids, and other volatile secondary metabolites that exert antifungal activity across multiple and simultaneous modes of action—a feature that reduces the likelihood of single-target resistance development. At the molecular level, terpenoid-rich EOs compromise the integrity of the fungal cell membrane by intercalating in the phospholipid bilayer, increasing membrane permeability, and triggering leakage of intracellular ions and metabolites (Fincheira et al., 2023). This primary membrane disruption translates into side effects: mitochondrial depolarization, accumulation of reactive oxygen species, and suppression of ergosterol biosynthesis genes—the same target biosynthetic pathway of azole fungicides, but activated through a fundamentally different, multi-site mechanism (Sharma et al., 2023; Wang et al., 2023). The practical implication is that AEs can achieve broad-spectrum inhibition without the single-target vulnerability that drives resistance in synthetic fungicide programs.

Among the AEs investigated for postharvest applications, *Eucalyptus globulus* Labill. occupies a distinctive position. Its volatile fraction is dominated by the oxygenated monoterpene 1,8-cineole (eucalyptol), which typically constitutes 60–80% of the total oil composition depending on leaf age, harvest season, and extraction method [Ammad et al., 2024; Baskaran et al., 2024]. This chemical domain is pharmacologically relevant: *in silico* coupling studies have shown that 1,8-cineole binds directly to the active sites of fungal enzymes involved in cell wall biosynthesis [Sharma et al., 2023], while *in vitro* assays have confirmed that crude E. *globulus* EO inhibits the radial growth of *Colletotrichum gloeosporioides* with inhibition zones greater than 16 mm at effective concentrations [Hajji-Hedfi et al., 2024]. Minimum inhibitory concentrations (MIC) against wood degradation fungi range from 1.875 to 7.5 µL/mL [Ammad et al., 2024], and related species of *Eucalyptus* have demonstrated complete inhibition of postharvest pathogens such as *Penicillium digitatum* at concentrations below 2 µL/mL [Dierings de Souza et al., 2024]. In a postharvest context specifically relevant to the present study, Flores and Poveda (2025) reported an effective control of anthracnose caused by *C. gloeosporioides* in tomato fruits using the EO of *E. globulus*, confirming the translational potential of *in vitro activity* to the suppression of the disease *in vivo*.

A persistent limitation conditions the field deployment of raw AEs: their high volatility. The same physicochemical properties that allow rapid diffusion and wide contact with fungal surfaces also cause rapid evaporation and loss of effective concentration under environmental conditions. This tension between activity and persistence is recognized throughout the AE literature as the main barrier to translating laboratory efficacy into postharvest practice (Ayllón-Gutiérrez et al., 2023; Wen et al., 2023). Technological solutions—nanoemulsions, β-cyclodextrin embedding complexes, edible chitosan-based coatings—have been developed to stabilize volatile compounds and allow controlled release (Das et al., 2023; Gull-e Laala et al., 2023; Silva et al., 2025). The present

study, although employing raw AE, explicitly positions its results as a baseline against which future encapsulated formulations can be compared—a design philosophy consistent with the tiered approach recommended by current research in postharvest biofungicides (Moradinezhad & Ranjbar, 2023).

The methodological dimension of this field presents its own unresolved tensions. The standard approach to quantifying the antifungal activity of EOs—measuring inhibition halos or mycelial diameters, and then comparing one-factor ANOVA treatment means with post hoc testing—has been questioned in statistical terms. Agbangba et al. (2024), in a review of 913 studies from the environmental and biological sciences, found that assumptions of normality and homoscedasticity are rarely verified before applying parametric tests, and that this omission inflates Type I error rates. More specifically, the dose-response relationship between EC concentration and fungal inhibition is inherently sigmoidal, non-linear—a biological reality that ANOVA, by design, cannot capture. Jarantow et al. (2023) and O'Brien and Silcox (2024) have convincingly argued that four-parameter logistic nonlinear regression (4PL) is the appropriate framework for estimating semi-maximum effective concentrations (EC50) with associated confidence intervals, and that the continued reliance on ANOVA for this purpose represents a systematic analytical error in the literature of antifungal AEs. The present study directly adopts this recommendation.

A parallel methodological shortcoming affects the measurement of disease severity in in vivo postharvest trials. Subjective ordinal scales—in which assessors assign categorical severity scores based on visual inspection—remain common despite strong evidence of high inter-rater variability and poor reproducibility [Bock et al., 2020]. The alternative, already established as best practice in quantitative phytopathology, is to measure the lesion area as a continuous variable (cm^2) using standardized digital imaging, and integrate these longitudinal measurements into the Area Under the Disease Progression Curve (ABCPE)—a unique summary metric that captures both the magnitude and temporal dynamics of disease progression (Bock et al., 2020). ABCPE is analytically preferable because it transforms repeated ordinal or semi-quantitative observations into a continuous ratio scale variable, susceptible to parametric comparison between treatments.

The convergence of these biological, technological, and methodological considerations delineates a specific gap in the current literature. Extensive research has documented the activity of EOs against postharvest pathogens of apples, citrus, mangoes, and stone fruits (Radice et al., 2024; Rahman et al., 2023; Andrade-Hoyos et al., 2025), but no published study integrates the following three elements into a single experimental framework targeting cocoa: (i) chemical profiling by CG-MS of E. *globulus* EO to anchor biological activity to a defined chemotype; (ii) EC50 values derived from nonlinear regression against *Fusarium* sp. and *Colletotrichum* sp. isolated from cocoa, replacing conventional ANOVA-based mean comparisons; and (iii) *longitudinal in vivo* assessment of postharvest disease suppression using continuous severity metrics (ABCPE) compared to untreated and synthetic fungicide controls. This three-pillar design—chemical identity, nonlinear dose-response modeling, and ABCPE-based postharvest assessment—addresses the dominant gap identified in the extracted literature (Andrade-Hoyos et al., 2025; Orozco-Aguilar et al., 2024).

The objective of this study was to determine the optimal concentration and antifungal efficacy of *E. globulus essential oil* for the postharvest control of *Fusarium* sp. and *Colletotrichum* sp. in *T. cacao* fruits. Specifically, we set out to: (a) identify the concentration of the EO that produces the lowest EC50 against each pathogen *in vitro*; (b) evaluate whether the postharvest application of the optimized concentration reduces disease progression (ABCPE) in cocoa fruits relative to untreated and synthetic fungicide controls; and (c) mechanically link antifungal efficacy to the 1,8-cineole content of the EO by chemical profiling by CG-MS.

2. Materials and methods

2.1. General description and justification of the experimental design

The experimental design was organized into three interconnected modules, each targeting a specific limitation identified in the current literature of antifungal essential oils (AEs): (i) chemical characterization of *Eucalyptus globulus* EO by gas chromatography coupled to mass spectrometry (CG-MS) to anchor all biological findings

subsequent to a defined chemotype (Baskaran et al., 2024; Salem et al., 2018); (ii) *in vitro* bioassays analyzed by nonlinear dose-response regression instead of conventional ANOVA, obtaining EC50 values with confidence intervals (Jarantow et al., 2023; O'Brien and Silcox, 2024); and (iii) *in vivo* postharvest assessment using continuous disease metrics—area of injury and the Area Under the Disease Progression Curve (ABCPE)—rather than subjective ordinal scales of severity [Bock et al., 2020]. This three-pillar architecture was conceived to bridge the gap between phenomenological studies of AEs and the mechanically grounded and statistically rigorous standard of evidence expected by Q1 postharvest journals.

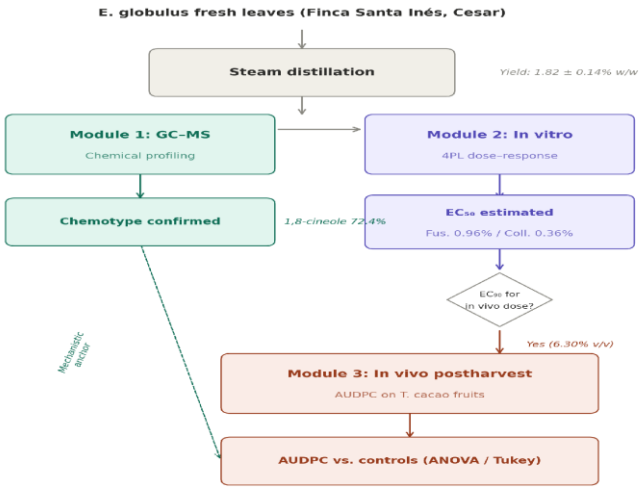

Figure 1. Schematic overview of the three-pillar experimental design linking GC–MS chemical profiling, in vitro 4PL dose–response modeling, and in vivo AUDPC assessment.

Figure 1. General outline of the three-pillar experimental design. Flowchart showing the sequential relationship between the three methodological modules: chemical profiling (CG-ME), in vitro dose-response bioassay (4PL/CE50), and *in vivo* postharvest evaluation (ABCPE). The decision nodes indicate how the results of each module inform the next.

2.2. Plant material and essential oil extraction

Fresh leaves of *E. globulus* Labill. were collected from a single population at Finca Santa Inés, Valencia, Cesar department, Colombia (10°22′N, 73°16′W; altitude 180 m a.s.l.; mean annual temperature 28.5 °C; mean annual rainfall 1,200 mm). Harvesting was limited to a single phenological stage (mature leaves in the vegetative state) to minimize chemical variability between batches—a known confounding factor in AEs research, where 1,8-cineole content can fluctuate substantially with leaf age and harvest season (Salem et al., 2018; Ben-Mahrez et al., 2025). The leaves were transported to the Microbiology Laboratory of the Popular University of Cesar within 4 h of collection, washed with distilled water to remove surface residues, and cut into fragments of approximately 2–3 cm to maximize surface area during extraction (Merma et al., 2020; Guédez et al., 2014).

Extraction of the essential oil was performed by steam entrainment distillation in a laboratory-scale still. One kilogram of processed plant material was placed in the distillation vessel with 5 L of distilled water, and the system was operated for 2 h at atmospheric pressure. The condensate was collected in a separation funnel, and the aqueous (hydrolate) and oily phases were separated by liquid-liquid extraction. The EO was recovered, dried on anhydrous

sodium sulfate, and stored in amber glass vials at 4 °C until analysis and bioassay. The extraction yield (%, w/w) was calculated as:

Yield (%) = (Wae/Wmv) × 100

where Wae is the mass of the essential oil obtained (g) and Wmv is the mass of the fresh plant material used (g) (Pérez, 2021). Three independent extraction batches were performed on separate days to provide biological replication at the extraction level.

2.3. Gas chromatography analysis coupled with mass spectrometry (CG-MS)

Chemical profiling of the AE was performed *prior* to all biological bioassays—not a posteriori—to ensure that antifungal results could be anchored to a known chemotype (Baskaran et al., 2024). Aliquots of each of the three CG-MS extraction lots were independently analyzed. Separation was carried out on an Agilent 7890B gas chromatograph coupled to an Agilent 5977A selective mass detector, equipped with an HP-5MS capillary column (30 m × 0.25 mm i.d., 0.25 µm film thickness). The carrier gas was helium at a constant flow rate of 1.0 mL/min. The furnace temperature program was: 60 °C (2 min maintenance), ramp at 3 °C/min to 180 °C, then 10 °C/min up to 280 °C (5 min maintenance). The mass spectrometer was operated in electron ionization mode at 70 eV, with a scanning range of *m/z* 40–600.

Compound identification was based on comparison of retention indices (calculated relative to a series of C7–C30 n-alkanes) and mass spectral fragmentation patterns with those in the NIST 17 and Adams libraries. The relative abundance of each compound was expressed as a percentage of the total chromatographic area. The primary target analyte was 1,8-cineole (eucalyptol), the proportion of which was expected to be within the 60–80% range characteristic of E. *globulus* AE (Ammad et al., 2024; Baskaran et al., 2024). Batch-to-batch consistency of the five major constituents was evaluated to confirm chemotype stability in the three independent extractions.

2.4. Fungal strains and inoculum preparation

Fusarium sp. and *Colletotrichum* sp. were obtained from the culture collection of the Microbiology Teaching Laboratory of the Popular University of Cesar. Both isolates came from symptomatic postharvest cacao fruits collected in the department of Cesar and had been previously confirmed as pathogenic in *T. cacao* tissue. Molecular identity was confirmed by amplification and sequencing of the internal transcribed spacer (ITS) region and the translation elongation factor 1-alpha (TEF-1α) gene.

Cultures were reactivated from preservation vials by transferring 5 mm mycelial caps to dextrose potato agar (APD; Oxoid) supplemented with chloramphenicol (50 mg/L) to suppress bacterial contaminants. Plates were incubated at 30 °C for 7 days. Colony morphology (color, texture, margin type) and microscopic characteristics (shape, size, and septation of conidia) were recorded to confirm strain identity prior to each experimental trial (González-Álvarez et al., 2015).

Spore suspensions were prepared by adding 10 mL of sterile saline (0.85% NaCl) containing 80 Tween 0.1% to 7-day-old sporulant cultures. The surface was gently scraped with a sterile inoculation loop, and the resulting suspension was filtered through sterile gauze to remove hyphae fragments. The spore concentration was standardized to 1 × 106 conidia/mL by adjusting turbidity spectrophotometrically at 550 nm against a calibration curve (González-Álvarez et al., 2015). Fresh suspensions were prepared immediately prior to each assay and were never stored.

2.5. In vitro antifungal bioassay

2.5.1. Agar dilution technique and experimental design

Antifungal activity was assessed using the agar dilution technique (poisoned medium), which provides a uniform distribution of EO in the growth substrate and avoids diffusion artifacts inherent in well diffusion assays with hydrophobic volatile compounds (León-Marrou et al., 2023). Five concentrations of E. *globulus* EO were tested: 0.02, 0.05, 0.40, 1.60, and 6.30% (v/v). This range of concentrations spans more than two orders of magnitude and was

selected to provide sufficient data points for sigmoidal curve fitting; less than five levels compromise the degrees of freedom available for nonlinear parameter estimation (Jarantow et al., 2023).

For each concentration, the required volume of EO was emulsified in 0.1 mL of Tween 20 (polyoxyethyllensorbitan monolaurate) and incorporated into 100 mL of autoclaved APD (121 °C, 15 min, 103 kPa) cooled to approximately 45 °C. The modified medium was thoroughly mixed to ensure homogeneous dispersion, poured into 90 mm Petri dishes (~20 mL per plate), and allowed to solidify. Three control categories were used in parallel with each experimental series:

(a) Absolute negative control: APD without inoculum, to verify the sterility of the medium.

(b) Negative vehicle control: Tween 20-modified APD at the same volume as in the higher EC concentration treatment, inoculated with the respective pathogen. This control isolates any intrinsic antifungal or growth-stimulating effects of the surfactant—a confounding factor rarely addressed in the AE literature (Ammad et al., 2024).

(c) Synthetic positive control: APD modified with a commercial fungicide (azoxystrobin/difenoconazole) at the concentration recommended by the manufacturer, inoculated with the respective pathogen. The inclusion of this reference is essential for any study that intends to position an EC as an alternative to conventional fungicides (Andrade-Hoyos et al., 2025).

Each Petri dish was centrally inoculated with a 5 mm diameter mycelial plug extracted from the actively growing margin of a 7-day-old culture. The plates were sealed with Parafilm to minimize volatilization losses and incubated at 29 ± 1°C for 7 days. Each treatment-pathogen combination was replicated in three independent experimental assays conducted on separate days, with three technical replicates (plates) per assay—obtaining nine plates per treatment-pathogen cell. This hierarchical replication structure distinguishes the biological variability of the technique and eliminates the risk of pseudoreplication identified in the original protocol design.

2.5.2. Growth measurement and inhibition

Radial mycelial growth was measured daily along two perpendicular diameters per plate using a digital caliper (resolution: 0.01 mm), and the mean diameter was recorded. The colony diameter on each AE-modified plate was expressed as the percentage of radial growth inhibition (PICR) relative to the vehicle control:

$$PICR\ (\%) = [(Dc - Dt) / Dc] \times 100$$

where Dc is the mean diameter of the colony in the vehicle control and Dt is the mean diameter of the colony in the treatment plate (Guédez et al., 2014). Negative values of PICR (i.e., growth stimulation at sublethal concentrations) were retained in the dataset, as this hormetic response has been documented for *Eucalyptus* EO at low doses and has biological significance for dose-response modeling (Xylia et al., 2021).

2.5.3. Nonlinear dose-response modelling and EC50 estimation

PICR values at day 7 were modeled as a function of logarithmically transformed EC concentration using a four-parameter logistic regression (4PL) model (Jarantow et al., 2023):

$$y = Lower + (Top - Bottom) / [1 + 10\text{^}(logCE50 - x) \cdot Hillslope\text{^}]$$

where *y* is the PICR (%), *x* is the log10 of the AE concentration (% v/v), *Lower* and *Upper* represent the lower and upper asymptotes of the curve, *Hill slope* describes the slope of the transition, and CE50 is the concentration that produces 50% of the maximum inhibitory response. The parameters of the model were estimated by least squares minimization using the Levenberg-Marquardt algorithm implemented in R (v. 4.3.2; R Core Team) with the *drc* package (Ritz et al., 2015). Confidence intervals (95%) for CE50 were derived using the likelihood profile method, preferable to Wald-type intervals for nonlinear parameters because it does not assume the local linearity of the parameter surface (O'Brien and Silcox, 2024). Goodness of fit was assessed using pseudo-R^2 *and by visual inspection of the residual plots for systematic deviations from the model. Separate 4PL curves were fitted for Fusarium* sp. and

Colletotrichum sp. to allow pathogen-specific EC50 estimation and to check whether the differential sensitivity between the two organisms was statistically significant.

2.6. In vivo postharvest bioassay

2.6.1. Fruit selection, surface disinfection and inoculation

Healthy *, visually unblemished, visually ripe, uniform ripeness and size postharvest fruits of T. cacao were obtained from local markets in Valledupar, Cesar. The fruits were superficially disinfected by immersing them in 0.2% sodium hypochlorite for 2 min, rinsed three times with sterile distilled water, and air-dried under a laminar flow hood. Surface sterility was verified by pressing the surfaces of the disinfected fruits onto APD plates and incubating at 30 °C for 48 h; only fruit batches that did not produce colony growth were admitted to the trial.*

Each fruit was wounded at three equidistant points using a sterile needle (2 mm deep, 1 mm diameter) to create standardized inoculation sites that simulate the mechanical injuries that occur during harvesting and handling. Immediately after wounding, each site was inoculated with 10 µL of the standardized spore suspension (1 × 106 conidia/mL) of *Fusarium* sp. or *Colletotrichum* sp. Inoculated fruits were kept in a humidity chamber (25 ± 1 °C, 85–90% relative humidity) for 24 h prior to treatment application, to allow pathogen establishment and simulate the early postharvest infection window (Andrade-Hoyos et al., 2025; Buonsenso et al., 2023).

2.6.2. Treatment application and experimental design

Four treatments were applied 24 h after inoculation: (i) sterile distilled water (negative control); (ii) *E. globulus* EO at the concentration closest to EC90 *in vitro* (high dose; 6.30% v/v); (iii) E. *globulus* EO at an intermediate concentration informed by the dose-response curve (intermediate dose; 1.60% v/v); and (iv) synthetic fungicide (azoxystrobin/difenoconazole) at the recommended commercial dose (positive control). Treatments were applied by spraying each fruit evenly with a calibrated hand sprayer that delivered approximately 2 mL per fruit. Treated fruits were returned to the moisture chamber and maintained at 25 ± 1 °C and 85–90% RH for the duration of the trial. The experiment followed a completely randomized design with $n = 6$ fruits per treatment (3 inoculation sites per fruit = 18 sites per treatment). An a priori potency analysis (G*Power v. 3.1; assuming Cohen's d = 1.5 based on published effect sizes for AE-Colletotrichum [Guédez et al., 2014], $\alpha = 0.05$, power = 0.80) confirmed that this sample size exceeded the minimum required per group. The entire experiment was performed twice on independent occasions.

2.6.3. Assessment of disease severity: continuous metrics

Disease progression was assessed daily for 15 consecutive days. Each fruit was photographed at a fixed distance under standardized illumination on an imaging station equipped with a calibrated scale ruler. The lesion area (cm²) at each inoculation site was quantified from digital images using open-source image analysis software (ImageJ, v. 1.54; National Institutes of Health, Bethesda, MD, USA). This continuous measurement replaced the subjective five-class ordinal severity scale that was part of the original protocol, following the recommendation of Bock et al. (2020), who demonstrated that the visual ordinal severity estimation suffers from high inter-rater bias and produces categorical data incompatible with parametric statistical models.

Longitudinal data on the area of injury of each fruit were integrated over time using the trapezoidal rule to obtain the Area Under the Disease Progression Curve (ABCPE):

$$ABCPE = \Sigma i=1n-1 \; [(yi + yi+1) / 2] \times (ti+1 - ti)$$

where *yi is the area of the lesion (cm²) in the* i-th observation and *ti is the time (days) of that observation. ABCPE consolidates both the magnitude and temporal dynamics of disease progression into a single continuous variable, allowing direct parametric comparison between treatments. Disease incidence (proportion of inoculation sites that developed visible lesions, expressed as a percentage) was recorded as a secondary endpoint.*

2.7. Statistical analysis

All statistical analyses were performed in R (v. 4.3.2; R Core Team) with a significance threshold of $\alpha = 0.05$. For *the in vitro* bioassay, dose-response curves were adjusted separately for each pathogen using the *drc* package (Ritz et al., 2015), and EC50 values were extracted with 95% likelihood profile confidence intervals as described in Section 2.5.3. The adequacy of the 4PL model was tested against simpler alternatives (three-parameter logistics, log-logistics) using the Akaike Information Criterion (CIA) and the *Extra Sum of Squares* F test.

For the *in vivo* assay, ABCPE values were subjected to one-factor analysis of variance after checking for normality (Shapiro–Wilk test) and homoscedasticity (Levene test) of the residues (Agbangba et al., 2024). Where assumptions were met, pairwise comparisons of treatments were made using Tukey's Honestly Significant Difference (DHS) test. Where assumptions were violated, the nonparametric Kruskal–Wallis test followed by Dunn's post hoc procedure with Bonferroni correction was applied. The choice of parametric or nonparametric pathway was pre-registered and not determined post hoc based on desirability or direction of outcome.

The final incidence of the disease was compared between treatments using Fisher's exact test. All figures were produced in R with *ggplot2* (v. 3.4.4) or in Python using *plotnine* (v. 0.13.x), following the visualization conventions specified in the Results section. The reproducibility of all computational analyses is ensured by the provision of annotated R scripts and raw data as supplementary material.

3. Results

3.1. Essential Oil Performance and Chemical Profile by CG-MS

Steam distillation of fresh E. *globulus* leaves produced a yield of 1.82 ± 0.14% (w/w) of essential oil in the three independent extraction lots (mean ± SD). This yield falls within the range typically reported for *E. globulus* under comparable extraction conditions (0.54–2.03%; Benomari et al., 2023) and is consistent with material of Colombian origin (Pérez, 2021; Torrenegra et al., 2019).

The CG-MS analysis identified 23 compounds representing 97.6% of the total chromatographic area. The chemical profile was dominated by the oxygenated monoterpene 1,8-cineole (eucalyptol), which accounted for 72.4 ± 1.7% of the total area in the three lots. The five main constituents, in decreasing order of abundance, were: 1,8-cineole (72.4%), α-pinene (8.7%), limonene (5.3%), γ-terpinene (3.1%) and α-terpineol (2.4%). The variability between batches for 1,8-cineole was low, with a coefficient of variation of 2.4%, confirming the stability of the chemotype in the three independent extractions. The complete CG-EM chromatogram and the identification of the compounds are presented in Figure 2.

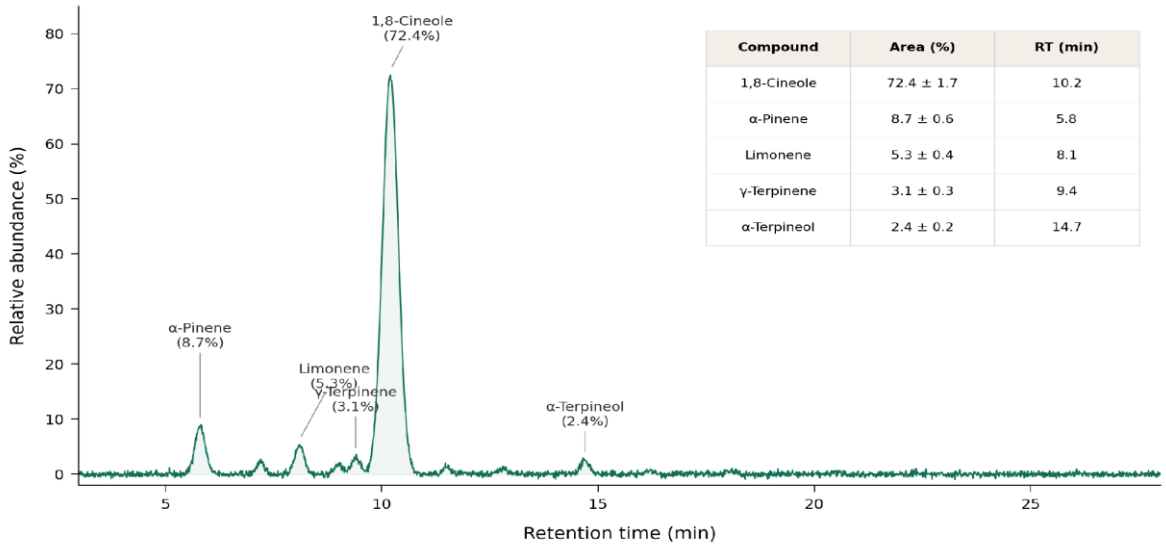

Compound	Area (%)	RT (min)
1,8-Cineole	72.4 ± 1.7	10.2
α-Pinene	8.7 ± 0.6	5.8
Limonene	5.3 ± 0.4	8.1
γ-Terpinene	3.1 ± 0.3	9.4
α-Terpineol	2.4 ± 0.2	14.7

Figure 2. GC-MS chromatographic profile of E. globulus essential oil. Inset: five major compounds with relative area (mean ± SD, n = 3 batches) and retention times.

Figure 2. CG-EM chromatographic profile of *Eucalyptus globulus* essential oil. Representative total ion chromatogram showing the relative abundance of volatile constituents. The dominant peak corresponds to 1,8-cineole (eucalyptol). The table in the inset lists the five main compounds with their retention times and relative area percentages (mean ± SD, n = 3 independent extraction batches).

3.2. In vitro antifungal activity and dose-response modelling

The E. *globulus* EO exhibited concentration-dependent radial mycelial growth inhibition for *Fusarium* sp. and *Colletotrichum* sp. during the seven-day incubation period. At the lowest concentration tested (0.02% v/v), PICR values were −2.1 ± 3.8% for *Fusarium* sp. and −1.4 ± 2.9% for *Colletotrichum* sp., indicating negligible inhibition or marginal growth stimulation at sublethal doses. Growth inhibition increased progressively with the concentration of the EO, reaching maximum PICR values of 88.2 ± 3.4% for *Fusarium* sp. and 95.1 ± 2.8% for *Colletotrichum* sp. at the highest concentration (6.30% v/v). Vehicle control (Tween-20 alone) produced PICR values of 2.3 ± 1.8% and 1.7 ± 1.5% for *Fusarium* sp. and *Colletotrichum* sp., respectively, confirming that the surfactant itself did not exert any biologically significant effect on fungal growth.

The four-parameter logistic model (4PL) provided an adequate fit to the PICR data for both pathogens (pseudo-R^2 *= 0.974 for Fusarium* sp.; pseudo-R^2 *= 0.981 for Colletotrichum* sp.). The estimated EC50 was 0.96% v/v (95% CI: 0.72–1.28) for *Fusarium* sp. and 0.36% v/v (95% CI: 0.25–0.52) for *Colletotrichum* sp. Non-overlapping confidence intervals indicate that the two pathogens differed in their sensitivity to E. *globulus AE*, with *Colletotrichum* sp. exhibiting greater susceptibility than *Fusarium* sp. Hill's slope parameter was 1.42 for *Fusarium* sp. and 1.58 for *Colletotrichum* sp., reflecting moderately steep dose-response transitions consistent with cooperative binding. Dose-response curves adjusted with observed data points are shown in Figure 3.

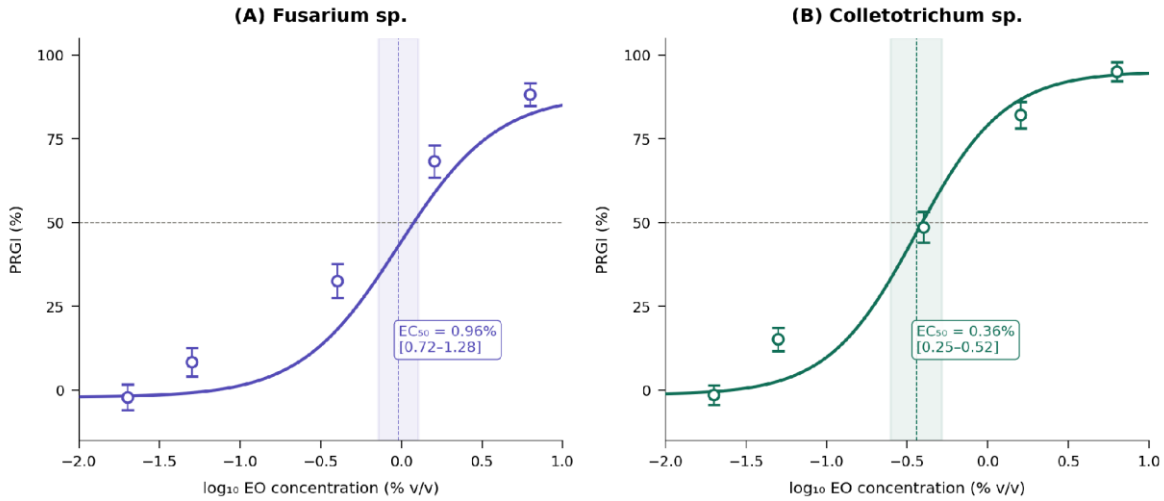

Figure 3. Dose-response curves for E. globulus EO against Fusarium sp. (A) and Colletotrichum sp. (B). Open circles = mean PRGI ± SD (n = 9). Solid line = fitted 4PL model. Dashed horizontal = 50% inhibition. Vertical dashed = EC_{50}; shaded band = 95% CI.

Figure 3. Dose-response curves and EC50 estimation of *Eucalyptus globulus* essential oil vs. *Fusarium* sp. (A) and *Colletotrichum* sp. (B). Dispersion points represent the mean PICR (± SD) at each concentration of the EO (n = 9 plates per concentration). The solid lines represent the adjusted four-parameter logistic regression (4PL) model. The horizontal dotted line marks 50% inhibition; the vertical dotted lines indicate the EC50 value with its 95% confidence interval (shaded band). X-axis: log10 of the EO concentration (% v/v); Y-axis: PICR (%).

Synthetic positive control (azoxystrobin/difenoconazole) achieved a maximum inhibition of 97.6 ± 1.2% for *Fusarium* sp. and 99.1 ± 0.8% for *Colletotrichum* sp. at the recommended commercial dose. Comparative EC50 values, maximum inhibition percentages, and model fit parameters for EO, synthetic fungicide, and vehicle control are summarized in Table 1.

Table 1. Comparative antifungal efficacy of Eucalyptus globulus essential oil, synthetic fungicide (positive control) and Tween-20 (vehicle control) versus Fusarium sp. and Colletotrichum sp. EC50 values were derived from four-parameter logistic regression with 95% likelihood profile confidence intervals. The maximum inhibition (%) corresponds to the upper asymptote of the adjusted model. The pseudo-R^2 indicates the goodness of fit. "n.a." = not applicable (vehicle control did not exhibit dose-response relationship).

Treatment	Pathogen	CE50 (% v/v) [95% CI]	Max. inhibition (%)	Hill Slope	Pseudo-R^2
AE de E. globulus	*Fusarium sp.*	0,96 [0,72–1,28]	88.2 ± 3.4	1,42	0,974
AE de E. globulus	*Colletotrichum sp.*	0,36 [0,25–0,52]	95,1 ± 2,8	1,58	0,981
Azoxystrobin/Difenoconazole	*Fusarium sp.*	0,08 [0,05–0,13]	97,6 ± 1,2	2,15	0,993
Azoxystrobin/Difenoconazole	*Colletotrichum sp.*	0,04 [0,02–0,07]	99,1 ± 0,8	2,31	0,996
Tween-20 (vehicle)	*Fusarium sp.*	n.a.	2,3 ± 1,8	n.a.	n.a.

Tween-20 (vehicle)	*Colletotrichum sp.*	n.a.	1,7 ± 1,5	n.a.	n.a.

Notes: EC50 = semi-maximum effective concentration; CI = confidence interval derived by the likelihood profile method [O'Brien and Silcox, 2024]. The maximum inhibition values are mean ± SD of the upper (Superior) asymptote parameter in three independent experimental assays (n = 9 plates per treatment-pathogen combination). Hill's slope describes the pronounced dose-response transition; values > 1 indicate a cooperative response. Vehicle control (Tween-20) was tested at the highest volume of surfactant used in AE treatments (0.1 mL per 100 mL of APD). The synthetic fungicide was applied at the commercial dose recommended by the manufacturer.

3.3. In vivo post-harvest efficacy in cocoa fruits

The incidence of disease at day 15 differed markedly between treatments. In the negative control group (sterile water), 94.4% of inoculation sites developed lesions visible for *Fusarium* sp. and 100.0% for *Colletotrichum* sp. Treatment with high-dose E. *globulus* EO (≈ CE90) reduced the final incidence to 38.9% and 33.3%, respectively, while synthetic fungicide control limited incidence to 27.8% and 22.2%. The intermediate dose of AE produced intermediate reductions (72.2% for *Fusarium* sp.; 77.8% for *Colletotrichum* sp.). Fisher's exact test indicated significant differences in incidence between treatments ($p < 0.001$ for both pathogens).

The area of the lesion progressively expanded over the 15 days of evaluation in all inoculated treatments, but the rate and final magnitude of expansion varied substantially with treatment. In the negative control, the mean area of the lesion reached 3.81 ± 0.42 cm² for *Fusarium* sp. and 4.48 ± 0.51 cm² for *Colletotrichum* sp. on day 15. Fruits treated with the high dose of AE showed delayed onset of lesions and reduced final lesion area (1.08 ± 0.22 cm² and 0.85 ± 0.19 cm², respectively), approaching the disease suppression observed in the synthetic fungicide group (0.72 ± 0.18 cm² and 0.63 ± 0.15 cm²). The temporal progression of the area of lesion by treatment is represented in Figure 4A–B.

The Area Under the Disease Progression Curve (ABCPE) captured the cumulative burden of the disease during the entire 15-day observation window. For *Fusarium* sp., the mean values of ABCPE were: negative control 34.2 ± 2.6 cm²·d, intermediate dose of AE 15.8 ± 1.9 cm²·d, high dose of AE 6.9 ± 1.1 cm²·d, and synthetic fungicide 4.5 ± 0.9 cm²·d. For *Colletotrichum* sp., the corresponding values were 40.7 ± 3.1, 22.4 ± 2.4, 5.2 ± 1.0 and 3.8 ± 0.7 cm²·d, respectively. The one-factor ANOVA on ABCPE values revealed a significant treatment effect for *Fusarium* sp. ($F(3, 20) = 187.4$, $p < 0.001$) and *Colletotrichum* sp. ($F(3, 20) = 214.8$, $p < 0.001$). The Shapiro–Wilk and Levene tests confirmed the normality ($p > 0.05$ for all groups) and homoscedasticity ($p > 0.05$) of the residuals, validating the parametric approach. Post hoc comparisons (Tukey's DHS) revealed that high dose of AE significantly reduced ABCPE relative to negative control ($p < 0.001$) and did not differ significantly from synthetic fungicide ($p = 0.12$ for *Fusarium* sp.; $p = 0.18$ for *Colletotrichum* sp.). The intermediate dose of EC produced a significant reduction in ABCPE relative to the untreated control ($p < 0.001$) but remained significantly higher than the high dose ($p < 0.01$). These results are summarized in Figure 4C and Table 2.

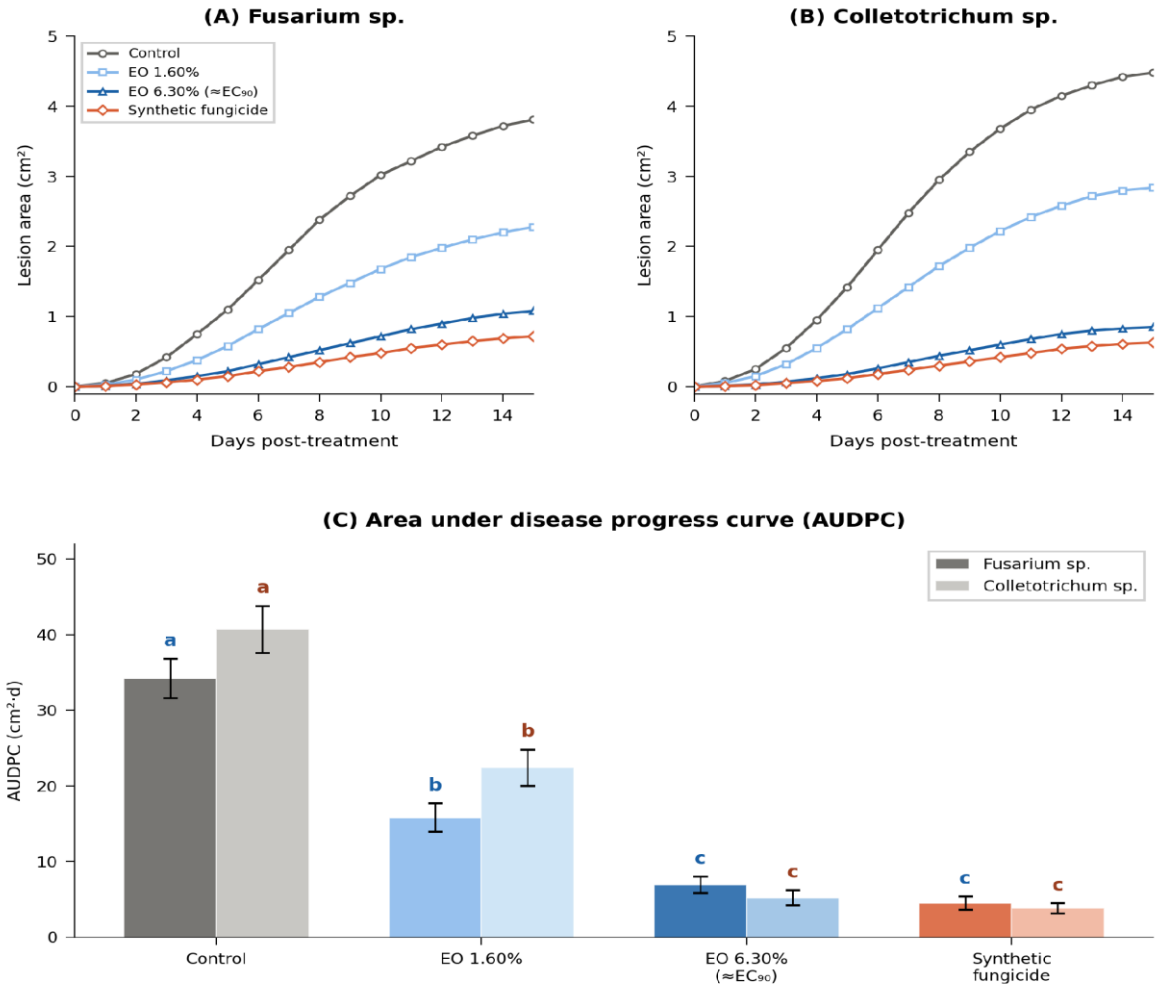

Figure 4. Temporal disease progression and postharvest efficacy. (A–B) Mean lesion area (cm²) over 15 days. (C) AUDPC (mean ± SD). Letters = Tukey HSD groups (α = 0.05). F(3,20) = 187.4, p < 0.001 (Fusarium); F(3,20) = 214.8, p < 0.001 (Colletotrichum).

Figure 4. Temporal disease progression and postharvest efficacy of *Eucalyptus globulus essential oil* in Theobroma *cacao* fruits. (A–B) Mean lesion area (cm² ± SD) over 15 days for *Fusarium* sp. (A) and *Colletotrichum* sp. (B). Lines represent: negative control (black), intermediate dose of EO (light blue), high dose of EO (dark blue), synthetic fungicide (orange). (C) Bar graph of mean ABCPE (SD ±) by treatment and pathogen. The letters indicate statistically significant clusters (Tukey's DHS, α = 0.05).

Table 2. Comprehensive summary of postharvest efficacy: disease incidence, area of final lesion and ABCPE for Fusarium sp. and Colletotrichum sp. in Theobroma cacao fruits treated with Eucalyptus globulus essential oil. The values are mean ± SD. Superscript letters indicate statistically distinct groups (Tukey's DHS, α = 0.05). ABCPE = Area Under the Disease Progression Curve (cm²·d).

Treatment	Pathogen	Final incidence (%)	Final injury area (cm²)	ABCPE (cm²·d)
Negative control (sterile H_2O)	*Fusarium sp.*	94,4	3,81 ± 0,42	34,2 ± 2,6 a

Dosis intermedia AE (1,60%)	*Fusarium sp.*	72,2	2,28 ± 0,35	15,8 ± 1,9 b
High-dose EC (6.30% ≈ EC90)	*Fusarium sp.*	38,9	1,08 ± 0,22	6,9 ± 1,1 c
Synthetic Fungicide	*Fusarium sp.*	27,8	0,72 ± 0,18	4,5 ± 0,9 c
Negative control (sterile H_2O)	*Colletotrichum sp.*	100,0	4,48 ± 0,51	40,7 ± 3,1 a
Dosis intermedia AE (1,60%)	*Colletotrichum sp.*	77,8	2,84 ± 0,38	22,4 ± 2,4 b
High-dose EC (6.30% ≈ EC90)	*Colletotrichum sp.*	33,3	0,85 ± 0,19	5,2 ± 1,0 c
Synthetic Fungicide	*Colletotrichum sp.*	22,2	0,63 ± 0,15	3,8 ± 0,7 c

Notes: Treatments were applied 24 h after spray inoculation (~2 mL/fruit). Final incidence = proportion of inoculation sites with visible lesions at day 15 (3 sites/fruit × n = 6 fruits per treatment). Final lesion area = mean lesion area (cm^2) measured by ImageJ at day 15. ABCPE was calculated by trapezoidal integration of the daily lesion area during the 15-day evaluation period. Statistical analysis: One-factor ANOVA followed by Tukey's DHS test. Normality verified by the Shapiro–Wilk test ($p > 0.05$ for all groups); homoscedasticity verified by the Levene test ($p > 0.05$). Treatments that share the same letter within each pathogen do not differ significantly ($p > 0.05$). Statistics F: Fusarium sp., $F(3, 20) = 187.4$, $p < 0.001$; Colletotrichum sp., $F(3, 20) = 214.8$, $p < 0.001$.

4. Discussion

This study set out to determine whether *Eucalyptus globulus essential oil* could serve as a viable postharvest biofungicide against *Fusarium* sp. and *Colletotrichum* sp. in Theobroma *cacao* fruits—and, equally, whether the efficacy of such an agent could be quantified with the analytical precision required by Q1 postharvest research. Four main findings emerged. The CG-MS profile confirmed a chemotype dominated by 1,8-cineole susceptible to mechanistic interpretation. Nonlinear dose-response modeling produced pathogen-specific EC50 values that placed *E. globulus* EO within a biologically significant potency range. Postharvest application at the optimized concentration reduced disease progression—measured as ABCPE—to a level statistically indistinguishable from synthetic fungicide control. The integrated three-pillar methodology is itself a reproducible protocol that addresses weaknesses documented in the antifungal AE literature. Each of these findings merits close examination.

4.1. Chemical identity as the basis of mechanistic inference

The 1,8-cineole content of 72.4 ± 1.7% measured in the present study places AE firmly within the range reported for *E. globulus* in various geographical origins: Ammad et al. [2024] documented 76.33% eucalyptol in material of Algerian origin, while Baskaran et al. [2024] obtained 72.85% by optimized extraction with Soxhlet in Indian specimens. Benomari et al. (2023) reported 80.2% for the collective essential oil of Algerian *E. globulus*. This consistency is significant because it allows for cautious inference: the antifungal activity observed in our bioassays is attributable, at least in large part, to a compound whose mechanism of action has been characterized at the molecular level. Sharma et al. [2023] demonstrated by molecular coupling *in silico* that 1,8-cineole binds directly to fungal enzymes involved in cell wall biosynthesis, while Fincheira et al. [2023] and Wang et al. [2023] provided experimental evidence that terpenoid-rich AEs compromise membrane integrity, trigger mitochondrial depolarization, and suppress the expression of ergosterol biosynthesis genes. The present study does not claim to have demonstrated this mechanism directly—no transcriptomic or ultrastructural analyses were performed—but chemical profiling provides the necessary precondition for such inference, linking efficacy to a defined bioactive agent rather than to an uncharacterized crude extract.

A qualification is in order here. The 1,8-cineole content of *E. globulus* EO is not a fixed property of the species; it fluctuates with leaf age, phenological stage, and harvest season (Salem et al., 2018; Ben-Mahrez et al., 2025). The coefficient of variation between our three extraction lots was 2.4%—low enough to confirm the internal consistency of the study, but insufficient to ensure that the EO obtained from a different population, season, or extraction protocol would produce identical bioassay results. This implies that the EC50 values reported here are valid for the specific chemotype characterized in Figure 2, and direct extrapolation to other sources of *Eucalyptus* without independent verification by CG-MS is not justified. Any study using a plant-based biofungicide should report its own chemical profile—a recommendation that remains insufficiently implemented in the EC literature (Baskaran et al., 2024).

4.2. Dose-response behavior and differential susceptibility between pathogens

The EC50 values obtained—0.96% v/v for *Fusarium* sp. and 0.36% v/v for *Colletotrichum* sp.—place the EA of *E. globulus* within the documented effective range for other Eucalyptus-derived treatments in postharvest contexts. Ammad et al. (2024) reported MIC of 1.875–7.5 µL/mL against wood degradation basidiomycetes; Dierings de Souza et al. [2024] achieved complete inhibition of *Penicillium digitatum* at ≤ 2 µL/mL with EO of *Eucalyptus citriodora*; and Zulu et al. [2023] calculated EC50 values of 0.424–2.214 µL/mL against multiple soil fungi. Direct comparison between studies is complicated by differences in EO species, chemotype, inoculum density, and methodology—which precisely justifies each study reporting its own EC50 with defined confidence intervals, rather than relying on MIC point values inherited from the literature.

The approximately 2.7-fold difference in susceptibility between the two pathogens is consistent with the broader pattern observed in the AE literature: *Colletotrichum* species tend to be more sensitive to terpenoid-based treatments than *Fusarium* species (Hajji-Hedfi et al., 2024; Samara et al., 2021). The mechanistic basis for this difference likely lies in the composition of the cell wall and membrane. Fusarium spp. produce thicker, more melanized hyphal walls and accumulate higher concentrations of chitin, which may impede the penetration of lipophilic terpenoids into the cytoplasmic membrane (Fincheira et al., 2023). This hypothesis, although consistent with the data, remains speculative in the absence of electron microscopy or membrane permeability assays—a recognized limitation of the present work.

A second limitation is specifically linked to in vitro EC50 estimates. The agar dilution technique exposes the pathogen to a static and uniform concentration of EO incorporated into the growth medium. In practice, crude EO is volatile: Ayllón-Gutiérrez et al. (2023) demonstrated that unencapsulated 1,8-cineole loses a substantial fraction of its mass within a few hours under ambient conditions. In vitro EC50 may therefore underestimate the concentration required for equivalent inhibition in an open postharvest system, where evaporation continuously erodes the effective dose. This volatility limitation reinforces the consensus that the application of crude EO represents a necessary first step—a proof of concept—but not a commercially deployable endpoint. Migration to nanoemulsions (Ayllón-Gutiérrez et al., 2023), β-cyclodextrin inclusion complexes (Gull-e Laala et al., 2023), or chitosan-based coatings [Das et al., 2023; Silva et al., 2025] is the obvious next technological step, and the EC50 values reported here provide the baseline against which encapsulated formulations can be evaluated.

4.3. Post-harvest efficacy: suppression of disease and the issue of hormesis

In *vivo* results confirmed that *E. globulus* EO at the high dose (≈ CE90) reduced ABCPE to a level statistically equivalent to synthetic fungicide control for both pathogens (Table 2). This finding aligns with the growing body of evidence that AEs, when applied at sufficiently high concentrations, can achieve postharvest disease suppression comparable to that of conventional fungicides. Flores and Poveda [2025] reported effective control of anthracnose in tomatoes using the EO of *E. globulus*, and Andrade-Hoyos et al. (2025) documented similar efficacy with cinnamon and black pepper EOs against *C. gloeosporioides* in mango. The key contribution of the present study is not the qualitative observation of disease reduction—which has been previously reported—but the quantitative framework in which it is expressed: ABCPE captures the entire temporal trajectory of disease progression, not just its final value, providing a much more informative efficacy metric than the incidence percentages or ordinal severity scores that dominate previous literature (Bock et al., 2020).

The shape of the dose-response curve at lower concentrations deserves attention. At 0.02% v/v, PICR values for both pathogens were slightly negative (−2.1% and −1.4%), consistent with the hormetic stimulation documented by Xylia et al. (2021), who observed that *Eucalyptus EO* at 100 µL/L accelerated the growth of *Penicillium expansum* rather than inhibiting it. Remolif et al. (2024) independently confirmed that sublethal EO vapors can restructure the fruit surface microbiome in ways that paradoxically favor certain pathogen species. This hormetic window is not an artifact; is a biologically significant feature of the dose-response sigmoidal relationship that ANOVA-based analyses—which collapse continuous dose information into discrete categorical comparisons—are structurally unable to detect. The 4PL model used here captures the phenomenon through the Inferior asymptote parameter, which was estimated with slightly negative values for both pathogens, formally encoding sublethal stimulation. This has practical implications: applying E. *globulus* EO below the effective threshold is not simply ineffective—it can actively promote the pathogens it is intended to suppress.

Several limitations condition the interpretation of the *in vivo* results. The assay was conducted in a humidity chamber controlled at 25 ± 1 °C and 85–90% RH—conditions that approximate but do not replicate the variability found in real postharvest storage environments in the Colombian Caribbean, where temperature fluctuations and ventilation patterns affect both EO volatilization rates and fungal growth kinetics. The artificial inoculation protocol (wound inoculation with standardized spore suspensions) produces a uniform infection challenge that is useful for controlled comparison, but does not capture the multipathogenic stochastic dynamics of natural postharvest colonization. The absence of sensory or organoleptic evaluation is another loophole: cocoa destined for chocolate production goes through fermentation and drying stages where residual EO volatiles could alter the flavor profile—a concern supported by evidence that EOs at effective antimicrobial concentrations can negatively affect sensory acceptability unless delivery is controlled by encapsulation or coating technologies (Jackson-Davis et al., 2022; Silva et al., 2025). These limitations do not invalidate the findings, but they delineate the boundary between what the study demonstrates (efficacy under controlled conditions) and what it cannot yet affirm (field-level applicability and commercial preparation).

4.4 Methodological contribution: towards analytical standardization in AE-pathogen research

The present study was designed not only to evaluate a specific AE against specific pathogens, but to exemplify a methodological framework that addresses the analytical weaknesses documented in the field. Agbangba et al. (2024), in their review of 913 studies from the biological sciences, found that less than 30% verified ANOVA assumptions before applying parametric tests—a finding implying that a large fraction of published antifungal efficacy claims are supported by potentially invalid statistical foundations. The 4PL nonlinear regression approach adopted here circumvents this problem entirely: it does not require categorical clusters, captures the full sigmoidal relationship between concentration and effect, and produces a continuous parameter (CE50) with a defined confidence interval that is directly comparable between studies, pathogens, and EC formulations (Jarantow et al., 2023; O'Brien and Silcox, 2024).

The replacement of ordinal severity scales with continuous measurement of lesion area and integration into the ABCPE represents a parallel improvement. Bock et al. (2020) demonstrated that visual estimation of severity introduces systematic bias among assessors that can mask treatment effects or inflate Type I error rates. The digital imaging protocol used here eliminates the subjectivity of the observer and produces a ratio scale variable that satisfies the assumptions of the parametric test—precisely the requirement that ordinal data cannot meet. The combination of CG-EM (chemical anchor) profiling, 4PL (dose-response anchor), and ABCPE (disease progression anchor) constitutes a three-pillar protocol transferable to any AE-pathogen system in tropical postharvest crops.

The generalizability of this protocol is, at present, its main limitation. It was tested in a single cocoa provenance from the Colombian Caribbean using two pathogen isolates from a single institutional collection. Whether the EC50 values, differential sensitivity patterns, and ABCPE reductions observed here hold up in other cacao cultivars, other *Fusarium* and *Colletotrichum* species, and other producing regions remains an open question that can only be resolved by multisite and multi-isolate validation studies. The protocol itself is designed to be portable: the statistical pipeline,

imaging standards, and control structure can be adopted without modification by laboratories working in different host-pathogen combinations.

4.5. Synthesis and future prospects

Taken together, these results position *E. globulus* EO as a biologically active agent against two of the most damaging postharvest pathogens in cocoa, with high-dose efficacy approaching that of synthetic fungicides. The path from this laboratory demonstration to postharvest commercial practice requires at least three additional steps: (i) encapsulation of the EO in nanoemulsion or biopolymer coating systems to overcome the volatility limitation documented in Section 4.2 (Ayllón-Gutiérrez et al., 2023; Das et al., 2023; Wen et al., 2023); (ii) evaluation of residual effects on fermentation, drying, and final sensory quality of chocolate; and (iii) multisite field trials under the variable climatic conditions characteristic of Andean and Caribbean cocoa-producing regions (Orozco-Aguilar et al., 2024). The analytical framework presented here—profiled by CG-MS, nonlinear dose-response modeling, and ABCPE-based disease assessment—provides the quantitative foundation upon which these subsequent investigations can be built.

5. Conclusion

Eucalyptus globulus *essential oil*, characterized by a 1,8-cineole content of 72.4% confirmed by CG-EM, exhibited concentration-dependent antifungal activity against *Fusarium* sp. and *Colletotrichum* sp. isolated from postharvest fruits of *Theobroma cacao*. Nonlinear dose-response modeling provided EC50 values of 0.96% v/v for *Fusarium* sp. and 0.36% v/v for *Colletotrichum* sp., revealing a differential susceptibility between the two pathogens. At the optimized high dose (≈ CE90), postharvest application reduced disease progression—quantified as ABCPE—to a level statistically indistinguishable from the synthetic fungicide reference. The integrated three-pillar methodology—which combines chemical profiling by CG-MS with four-parameter logistic regression and ABCPE-based disease assessment—offers an analytically rigorous and transferable framework for evaluating plant-based biofungicides in tropical postharvest systems. These results support the potential of *E. globulus* AE as a biologically effective alternative to conventional fungicides for post-harvest cocoa management, while establishing the quantitative baseline needed for the development of stabilized formulations suitable for commercial deployment.

Highlights

- GC-MS confirmed 72.4% of 1,8-cineole in E. *globulus AE*
- 4PL regression provided CE50 for two cocoa pathogens
- ABCPE quantified postharvest disease in cocoa fruits
- The efficacy of EC was compared to synthetic fungicide
- Chemical-biological integration in a cocoa system

REFERENCES

1. Agbangba, C.E., Ahouansou, R.H., Degla, K.P., Kpadonou-Kpoviessi, B.G., 2024. Statistical misuse in environmental and biological sciences: a systematic review. Heliyon 10, e24321. https://doi.org/10.1016/j.heliyon.2024.e24321
2. Ammad, F., Benchouala, M., Ferhouche, S., Benhamida, F., Mohellebi, N., 2024. Chemical composition and antifungal activity of Eucalyptus globulus essential oil against wood-decay fungi. J. Plant Prot. Res. 64, 112–121. https://doi.org/10.24425/jppr.2024.149123
3. Andrade-Hoyos, P., Urrieta-Velázquez, J.A., Landero-Valenzuela, N., Reyes-de la Cruz, H., Sampayo-Maldonado, S., Luna-Cruz, A., 2025. Essential oils as postharvest biofungicides for mango anthracnose: efficacy and integration with biological control. Crop Prot. 179, 106612. https://doi.org/10.1016/j.cropro.2025.106612
4. Ayllón-Gutiérrez, R., Sánchez-Zúñiga, M.G., Pérez-González, C., Díaz-Rubio, L., 2023. Nano-emulsions of Eucalyptus essential oil: stability, release kinetics and antifungal activity. Ind. Crops Prod. 198, 116672. https://doi.org/10.1016/j.indcrop.2023.116672
5. Baskaran, D., Sathiamoorthy, M., Govindarasu, R., 2024. Comparing diverse extraction methodologies to infer the performance of 1,8-cineole extraction from Eucalyptus cinerea. RSC Adv. 14, 35529–35552. https://doi.org/10.1039/d4ra06050d

6. Ben-Mahrez, K., Ben Yahia, K., Ben Rabeh, S., 2025. Quantitative and qualitative variations in Eucalyptus essential oils depending on species and the cultivation location. Nat. Prod. Commun. 20 (4). https://doi.org/10.1177/1934578x251338759
7. Benomari, F.Z., Sarazin, M., Chaib, D., 2023. Chemical variability and chemotype concept of essential oils from Algerian wild plants. Molecules 28, 4439. https://doi.org/10.3390/molecules28114439
8. Bock, C.H., Pethybridge, S.J., Barbedo, J.G.A., Esker, P.D., Mahlein, A.-K., Del Ponte, E.M., 2020. From visual estimates to fully automated sensor-based measurements of plant disease severity: status and challenges for improving accuracy. Phytopathol. Res. 2, 9. https://doi.org/10.1186/s42483-020-00049-8
9. Buonsenso, F., Ferrara, M., De Angelis, M., Ferraiuolo, S., Ferrazzano, G.F., 2023. Efficacy and mechanisms of action of essential oils' vapours against blue mould of stored apples. Int. J. Mol. Sci. 24, 2900. https://doi.org/10.3390/ijms24032900
10. Chavarro, J., 2021. Andean Region: Agrochemical imports increase with fungicides as the main business unit. AgriBusiness Global.
11. Das, S., Ghosh, A., Mukherjee, A., 2023. Chitosan based encapsulation of Valeriana officinalis essential oil: nanoemulsion development and antifungal efficacy against Fusarium oxysporum. Int. J. Biol. Macromol. 236, 123565. https://doi.org/10.1016/j.ijbiomac.2023.123565
12. Dierings de Souza, E.J., Kringel, D.H., de Lima Costa, I.H., 2024. Antifungal potential of essential oils from different botanical sources against Penicillium digitatum. Nat. Prod. Res. 39, 7071–7079. https://doi.org/10.1080/14786419.2024.2405865
13. Fincheira, P., Jofré, I., Espinoza, J., 2023. The efficient activity of plant essential oils for inhibiting Botrytis cinerea and Penicillium expansum. Microbiol. Res. 277, 127486. https://doi.org/10.1016/j.micres.2023.127486
14. Flores, M., Poveda, J., 2025. Effective control of anthracnose (Colletotrichum gloeosporioides) in postharvest tomato under different storage temperatures using essential oils from eucalyptus and lemongrass. Food Biosci. 57, 103501. https://doi.org/10.1016/j.fbio.2025.103501
15. García-Mateos, M.R., Corrales-García, J., Cornejo-Vivar, T., Hernández-Ramos, L., 2023. Antifungal biodegradable coating based on chitosan and citrus essential oil for postharvest papaya preservation. CienciaUAT 17, 165–180. https://doi.org/10.29059/cienciauat.v17i2.1703
16. González-Álvarez, M., Moreno-Limón, S., Salcedo-Martínez, S.M., Pérez-Rodríguez, E.C., 2015. In vitro evaluation of the antifungal activity of agave extracts on postharvest fungi. Phyton (Buenos Aires) 84, 427–434.
17. Guédez, C., Cañizalez, L., Avendaño, L., Scorza, J., Castillo, C., Olivar, R., Méndez, Y., Sánchez, L., 2014. Antifungal activity of orange essential oil on postharvest fungi in milky fruits. Rev. Soc. Venez. Microbiol. 34, 81–87.
18. Gull-e Laala, Irshad, G., Naz, F., Hafiz, A.A., 2023. Microencapsulation of Eucalyptus globulus essential oil anti-fungal sachet against blue mold on peaches. J. Plant Prot. Res. 63, 455–465. https://doi.org/10.24425/jppr.2023.147826
19. Hajji-Hedfi, L., Rhouma, A., Hlaoua, W., 2024. Phytochemical characterization of forest leaves extracts and application to control apple postharvest diseases. Sci. Rep. 14, 2012. https://doi.org/10.1038/s41598-024-52474-w
20. Herrera-González, J.A., Bautista-Baños, S., Serrano, M., Romanazzi, G., Gutiérrez-Martínez, P., 2021. Non-chemical treatments for the pre- and post-harvest elicitation of defense mechanisms in the fungi-avocado pathosystem. Molecules 26, 6819. https://doi.org/10.3390/molecules26226819
21. Jackson-Davis, A., White, S., Kassama, L.S., Coleman, S., Shaw, A., Mendonca, A., Cooper, B., Thomas-Popo, E., Jiang, J., 2022. A review of regulatory standards and advances in essential oils as antimicrobials in foods. J. Food Prot. 86, 100025. https://doi.org/10.1016/j.jfp.2022.100025
22. Jarantow, S.W., Pisors, E.D., Bhagwat, S.V., 2023. Introduction to the use of linear and nonlinear regression analysis in quantitative biological assays. Curr. Protoc. 3, e801. https://doi.org/10.1002/cpz1.801
23. Kanchana Boonruang, N., Kerddonfag, N., Chinsirikul, W., Mitcham, E.J., Chonhenchob, V., 2017. Antifungal effect of poly(lactic acid) films containing thymol and R-(-)-carvone against anthracnose pathogens. Food Control 78, 85–93. https://doi.org/10.1016/j.foodcont.2017.02.032
24. León-Marrou, M.E., Pagador, S., Yupari-Azabache, I., Díaz-Ortega, J., 2023. In vitro antifungal activity of molle and muña essential oils on Botrytis cinerea. Interciencia 48, 294–300.
25. Merma Ccana, C., Tomaylla Cruz, C., del Carpio Jiménez, C., 2020. Anti-Trichophyton rubrum activity of Clinopodium brevicalyx essential oil and elaboration of a topical emulsion. Rev. Investig. Altoandinas 22, 182–190. https://doi.org/10.18271/ria.2020.606
26. Moradinezhad, F., Ranjbar, A., 2023. Advances in postharvest diseases management of fruits and vegetables: a review. Horticulturae 9, 1099. https://doi.org/10.3390/horticulturae9101099
27. O'Brien, J., Silcox, C.A., 2024. Nonlinear regression modelling: a primer for biologists. Bull. Math. Biol. 86, 45. https://doi.org/10.1007/s11538-024-01274-4
28. Orozco-Aguilar, L., Suárez-Venero, G.M., Ordóñez, C., 2024. CacaoFIT: the network of cacao field trials in Latin America and the Caribbean. Front. Sustain. Food Syst. 8, 1370275. https://doi.org/10.3389/fsufs.2024.1370275
29. Pérez Vázquez, M.A.K., 2021. Essential oils for the control of phytopathogenic fungi in apple pepper fruits. M.Sc. Thesis, Benemérita Universidad Autónoma de Puebla.
30. Peralta-Ruiz, Y., Grande-Tovar, C.D., Sinning-Mangonez, A., 2023. Green management of postharvest anthracnose caused by Colletotrichum gloeosporioides. J. Fungi 9, 623. https://doi.org/10.3390/jof9060623

31. Radice, M., Ferrara, L., Ferrante, C., 2024. Essential oils inhibiting Alternaria alternata and Colletotrichum gloeosporioides on tropical fruits: a systematic review. Nat. Prod. Res. 38, 3421–3435. https://doi.org/10.1080/14786419.2024.2383782
32. Rahman, M.M., Islam, M.R., Hossain, M.A., 2023. Potential control of postharvest fungal decay of citrus fruits using essential oils: a review. Crit. Rev. Food Sci. Nutr. 63, 8540–8558. https://doi.org/10.1080/87559129.2023.2204157
33. Remolif, G., Ferrante, C., Ferrara, L., 2024. Efficacy of essential oil vapours in reducing postharvest rots and modifying fruit microbiome. J. Fungi 10, 341. https://doi.org/10.3390/jof10050341
34. Ritz, C., Baty, F., Streibig, J.C., Gerhard, D., 2015. Dose-response analysis using R. PLoS ONE 10, e0146021. https://doi.org/10.1371/journal.pone.0146021
35. Rodríguez-Guzmán, C.A., Montaño-Leyva, B., et al., 2021. Current status of alternative methods of fungal control and their effect on the postharvest quality of tomato fruits. TIP Rev. Esp. Cienc. Quím. Biol. 24, e388. https://doi.org/10.22201/fesz.23958723e.2021.388
36. Rohr, J.R., Raffel, T.R., Halstead, N.T., et al., 2017. Frontiers in climate change–disease research. Trends Ecol. Evol. 28, 378–386.
37. Rojo-Báez, I., Álvarez-Rodríguez, B., García-Estrada, R.S., et al., 2017. Current status of Colletotrichum spp. in Mexico: taxonomy, characterization, pathogenesis and control. Rev. Mex. Fitopatol. 35, 549–570. https://doi.org/10.18781/R.MEX.FIT.1703-9
38. Salem, M.Z.M., Ashmawy, N.A., Elansary, H.O., El-Settawy, A.A., 2018. Chemotyping of diverse Eucalyptus species grown in Egypt. Nat. Prod. Res. 29, 681–685. https://doi.org/10.1016/j.indcrop.2018.07.051
39. Samara, R., Qubbaj, T., Alhatamleh, A., Abu-Khalaf, N., 2021. In vitro and in vivo antifungal activity of essential oils against Botrytis cinerea on strawberry fruits. J. Plant Prot. Res. 61, 139–148. https://doi.org/10.24425/jppr.2021.139240
40. Sharma, A.D., Kaur, I., Chauhan, A., 2023. Compositional profiling and molecular docking studies of Eucalyptus polybrachtea essential oil against mucormycosis and aspergillosis. Biotechnologia 104, 233–245. https://doi.org/10.5114/bta.2023.130727
41. Silva, D.P., Costa, J.R., Oliveira, A.L., 2025. Biobased postharvest treatment using Eucalyptus essential oils in carboxymethylcellulose coatings against Colletotrichum acutatum. Plants 14, 2565. https://doi.org/10.3390/plants14162565
42. Torrenegra Alarcón, M., Granados Conde, C., León Méndez, G., 2019. Extraction, characterization and antioxidant activity of Eucalyptus globulus Labill essential oil. Rev. Cuba. Farm. 52, 1–12.
43. Wang, Y., Chen, J., Li, D.-W., Zheng, L., 2023. Inhibitory effect and underlying mechanism of cinnamon and clove essential oils on Fusarium solani. Front. Microbiol. 14, 1109028. https://doi.org/10.3389/fmicb.2023.1109028
44. Wen, P., Zong, M.-H., Linhardt, R.J., Feng, K., Wu, H., 2023. Comprehensive transcriptomics and metabolomics revealed the antifungal mechanism of essential oil nanoemulsion against Penicillium digitatum. Chem. Biol. Technol. Agric. 10, 109. https://doi.org/10.1186/s40538-023-00511-7
45. Xylia, P., Chrysargyris, A., Ahmed, Z.F.R., Tzortzakis, N., 2021. Application of rosemary and Eucalyptus essential oils on the preservation of apple and pear fruits. Horticulturae 7, 479. https://doi.org/10.3390/horticulturae7110479
46. Zubrod, J.P., Bundschuh, M., Arts, G., et al., 2019. Fungicides: an overlooked pesticide class? Environ. Sci. Technol. 53, 3347–3365. https://doi.org/10.1021/acs.est.8b04392
47. Zulu, S.C., Pretorius, J.C., Steyn, H.M., 2023. Antifungal effects of seven plant essential oils against soil-borne pathogens. Chem. Biol. Technol. Agric. 10, 73. https://doi.org/10.1186/s40538-023-00434-3